Acknowledgment. The author is grateful to K. Valentin for the measurement of the ^{31}P NMR spectra and to J. H. Bright, W. F. Herbes, and S. M. Gerber for helpful discussions.

References and Notes

(1) J. D. Guthrie, G. L. Drake Jr., and W. A. Reeves, *Am. Dyest. Rep.*, **44**, 328 (1955).
(2) W. A. Reeves and J. D. Guthrie, *Ind. Eng. Chem.*, **48**, 64 (1956).
(3) L. M. Fodor, Ph.D. Thesis, Cornell University, Ithaca, N.Y., 1963.
(4) J. K. De Jong and J. De Jonge, *Recl. Trav. Chim. Pays-Bas*, **71**, 643 (1952).
(5) A. Rakowski, *Z. Phys. Chem.*, **57**, 321 (1906).
(6) P. J. Flory, "Principles of Polymer Chemistry", Cornell University Press, Ithaca, N.Y., 1953, p 347.

Cobalt(III)-Promoted Hydrolysis of a Phosphate Ester

Bryan Anderson, Ronald M. Milburn,[1] John MacB. Harrowfield, Glen B. Robertson, and Alan M. Sargeson*

Contribution from the Research School of Chemistry, Australian National University, Canberra, A.C.T. 2600, Australia. *Received September 28, 1976*

Abstract: Chelated *p*-nitrophenylphosphatobis(trimethylenediamine)cobalt(III) perchlorate hydrolyses in the pH range 6.5–13.5 to ~35% *p*-nitrophenol and ~65% monodentate *p*-nitrophenylphosphate with a rate law, $k_{obsd} = k_1 + k_2[OH^-]$, $\mu = 0.5$, 25 °C where $k_1 = 7 \times 10^{-5}$ s^{-1} and $k_2 = 5.1$ M^{-1} s^{-1}. Tracer studies indicate that ester cleavage and chelate opening on the metal ion occur by different paths, through the chelated five-coordinate phosphorane intermediate and the conjugate base hydrolysis mechanism for Co(III) amine complexes, respectively. The ester hydrolysis is accelerated 10^9-fold relative to the uncoordinated ester in basic solution. Evidence for strain in the four-membered ring of the chelated ester is adduced from an x-ray crystallographic analysis of phosphatobis(ethylenediamine)cobalt(III) which is also reported. The results are discussed in relation to alkaline phosphatase activity.

One of the striking observations in biological phosphate chemistry is that it all appears to be metal ion catalyzed. However, the role of the metal ion in promoting biological hydrolysis reactions of phosphate derivatives including phosphate esters has been the subject of considerable speculation.[2-6] Some experimental approaches have involved model systems in which the relationship between the metal ion and the phosphate derivative has been difficult to define and in which the catalytic effects have been modest.[3]

The idea that chelate formation between a phosphate ester and a metal ion could result in greatly enhanced hydrolysis rates was conceived at least by Farrell, Kjellstrom, Spiro,[3] and ourselves after the extraordinarily high reactivity for five-membered cyclic phosphate esters was observed.[7] However, a tractable and unequivocal system to demonstrate this hypothesis has proved difficult to find and characterize. The experiments in this area,[3] with methyl phosphate and ethylenediamine and triethylenetetraminecobalt(III) complexes have displayed relatively small acceleratory effects over free methyl phosphate and there are many mechanistic ambiguities. We report here on the hydrolytic reactivity of *p*-nitrophenylphosphate in the chelate (*p*-nitrophenylphosphato)bis(trimethylenediamine)cobalt(III) cation, $[Co(tn)_2O_3POC_6H_4NO_2]^+$, a complicated but tractable system.

We have not discovered any structural studies of bidentate covalently bound phosphate complexes. Consequently we report an x-ray crystal structure analysis of phosphatobis(ethylenediamine)cobalt(III) which defines the geometry of the four-membered chelated phosphate ring and is relevant to the hydrolysis study.

Experimental Methods

Visible-UV spectra and rate data were collected on a Cary-118 recording spectrophotometer. ^1H NMR spectra were obtained at 100 MHz on a JEOL Minimar spectrometer. pH measurements were made with a Radiometer pH meter 26 using a sodium chloride salt bridge, with standardizations before and after measurements.

Analytical reagents were used in kinetic studies, except where otherwise specified. *p*-Nitrophenylphosphate, disodium salt, hexahydrate (Gold Label, 99%) was obtained from Aldrich Chemical Co. Sodium hydroxide solutions were freshly prepared from May and Baker "Volucon" concentrate, using carbon dioxide free water.

***trans*-$[Co(tn)_2(OH)(OH_2)](ClO_4)_2$** was prepared from $[Co(tn)_2CO_3]ClO_4$ in accord with the procedure of Jonasson et al.[8]

Anal. Calcd for $CoC_6H_{23}N_4Cl_2O_{10}$: C, 16.34; H, 5.26; N, 12.70. Found: C, 16.3; H, 5.2; N, 12.5.

***trans*-$[Co(tn)_2Cl_2]ClO_4$** was prepared by heating excess ~6 M aqueous hydrochloric acid and *trans*-$[Co(tn)_2(OH)(OH_2)](ClO_4)_2$ on a steam bath for ~30 min. After cooling, aqueous perchloric acid (~4 M) was added. The green product was collected and washed with dilute aqueous perchloric acid followed by ethanol and then ether before drying it over phosphorus pentoxide in vacuo.

$[Co(tn)_2O_3POC_6H_4NO_2]ClO_4$. Stoichiometric quantities of silver perchlorate (BDH, LR) and *p*-nitrophenylphosphate, disodium salt, hexahydrate, were mixed in aqueous solution to precipitate $Ag_2[O_3POC_6H_4NO_2]$. The product was washed with cold water and dried, in the dark, in vacuo over phosphorus pentoxide (~80% yield). $Ag_2[O_3POC_6H_4NO_2]$ (2.02 g, finely ground), *trans*-$[Co(tn)_2Cl_2]ClO_4$ (1.76 g), and Me_2SO (30 mL) were stirred (in a stoppered flask) at 20 °C in the dark. After ~10 min the solution became violet. Stirring was continued for ~18 h before removing the AgCl. The product was precipitated with dry ethanol and ether, filtered with minimum exposure to air, and washed with ethanol and then ether. Purification was achieved by dissolving it in a small volume of Me_2SO (~5 mL) and reprecipitating with aqueous $NaClO_4$ (0.25 M, 50 mL). The violet crystalline product was washed with aqueous $NaClO_4$, then with ethanol followed by ether, after which it was dried in vacuo over phosphorus pentoxide (~30% yield).

Anal. Calcd for $CoC_{12}H_{24}N_5PClO_{10}$: C, 27.52; H, 4.62; N, 13.37; P, 5.91; Cl, 6.77. Found: C, 27.6; H, 4.7; N, 13.2; P, 5.6; Cl, 6.5.

The ^1H NMR spectrum of $[Co(tn)_2O_3POC_6H_4NO_2]ClO_4$ in Me_2SO-d_6 gave the following chemical shifts (parts per million downfield from external Me_4Si; relative peak areas in parentheses): α-CH_2, 1.49 (8); β-CH_2, 2.47 (4); NH_2, 3.65 and 3.89 (overlapping, total 4); NH_2, 4.88 (2); aromatic H, doublet centered at 7.23 (2); NH_2, 7.89, and aromatic H, doublet centered at 8.10 (overlapping, total 4).

Analysis of *p*-Nitrophenylphosphate. A sample of $[Co(tn)_2O_3POC_6H_4NO_2]ClO_4$ (0.027 g) was dissolved directly in 2 M NaOH (10 mL). After 2 min ($>8t_{1/2}$ for hydrolysis) the solution was diluted 25-fold and a spectral measurement on an aliquot showed 7% *p*-nitrophenolate released, (based on the weight of complex). The re-

maining solution was passed through a cation exchange column, (Bio Rad, 50W × 2, 200–400 mesh, H^+ form) which was then washed carefully with water. The hydrogen ion concentration of the effluent solution together with washings was brought to 1 M with HCl and the mixture heated to 100 °C for 4 h to hydrolyze the remaining *p*-nitrophenylphosphate to *p*-nitrophenol.[9] The cooled solution was made alkaline with NaOH and spectral analysis of this solution revealed the available *p*-nitrophenylphosphate to be 97% of the theoretical amount.

Products of Base Hydrolysis of $[(tn)_2CoO_3POC_6H_4NO_2]ClO_4$. The complex, at a concentration $\sim 5 \times 10^{-4}$ M, was allowed to react for $10t_{1/2}$ (i.e., 30 s) for *p*-nitrophenolate release in 0.010 M NaOH. The reaction mixture pH was reduced to ~6 by addition of acetate buffer and the cationic species, then present, separated by chromatography on Na^+ SP SEPHADEX C25 (using $NaClO_4$ eluants buffered to pH ~ 5.5 with 5×10^{-3} M acetate buffer). Three pink-violet species were seen. The first was readily eluted with 0.1 M $NaClO_4$ and smeared on the column. Analysis showed it to contain the bulk of still coordinated p-nitrophenylphosphate. The second band moved slowly with 0.1 M $NaClO_4$ and seemed to react during the period of elution (bleeding forward, as if producing band 1 material). It was a minor component, but contained a significant amount of coordinated *p*-nitrophenylphosphate. The third band required 0.2 M $NaClO_4$ for its ready removal and contained no *p*-nitrophenylphosphate. In detail, the experimental procedure was as follows.

The complex (26 mg) was dissolved rapidly by stirring the solid in NaOH (10 mL, 0.010 M). After 30 s, 5 mL of 0.5 M 1:1 HOAc/OAc^- buffer was added to reduce the pH to ~6. The solution was absorbed as quickly as possible on a short column of Na^+ SP SEPHADEX C25 with gentle suction, the reaction flask being rinsed with 50 mL of H_2O. After absorption the column was washed with 75 mL of H_2O and the initial effluent, rinse effluent, and water wash were combined. A final wash (50 mL) was kept separate and analyzed to see if all nitrophenol and nitrophenylphosphate had been washed from the column. Elution with 0.1 M and then 0.2 M $NaClO_4$ was carried out to reveal three pink-violet species. All eluates were analyzed for nitrophenylphosphate by heating aliquots with 1 M HCl for 4 h at 100 °C, adding excess NaOH and recording the absorbance due to nitrophenolate (400 nm, ϵ 18 700 M^{-1} cm^{-1}). The initial effluent plus H_2O wash was analyzed for nitrophenylphosphate and nitrophenol by measuring the nitrophenol absorbance on a basicified aliquot before and after acid hydrolysis.

A duplicate experiment was conducted in which the quenched reaction mixture was adsorbed under gravity on the resin in the hope that this would lead to less smearing of the first complex band, but in the much longer time then required for chromatographic treatment it seemed that considerable reaction had occurred.

^{18}O Tracer Experiment. $[Co(tn)_2(O_3POC_6H_4NO_2)]ClO_4$ (0.5 g) was suspended in 0.1 M NaOH (10 mL) containing ~5 atom % $^{18}OH_2$ for 5 min at 25 °C. Over this period the complex largely dissolved with rapid formation of free nitrophenolate and free *p*-nitrophenylphosphate ions. The solution was sampled and ^{18}O enriched water distilled under vacuum. $Ba(ClO_4)_2$ (0.5 g) was added to the filtered solution to precipitate the nitrophenylphosphate cleaved from the Co complex. After 10 min the barium nitrophenylphosphate was collected, washed several times with ice water and dried in vacuo over P_2O_5 for 2 days. Anal. Calcd for $C_6H_4O_6NPBa$: P, 8.74; Ba, 38.75. Found: P, 8.8; Ba, 37.5.

Barium nitrophenylphosphate (~50 mg) was heated with an $HgCl_2/Hg(CN)_2$ mixture for 12 h at 400 °C. The condensable gases were then passed through a gas chromatograph and the CO_2 trapped. The solvent distilled from the reaction mixture (1 mL) was equilibrated with CO_2 (~2 mL) of normal enrichment at 70 °C. The CO_2 samples were then analyzed using a Mass Atlas M86 mass spectrometer to detect the 46:44 mass ratio, normal CO_2 $R = 0.004028$; solvent enriched CO_2 $R = 0.09613$; phosphate enriched CO_2 $R = 0.005242$.

Kinetics. The majority of kinetic measurements were in aqueous solution at 25.0 ± 0.05 °C and an ionic strength (μ) of 0.5 M, with $NaClO_4$, or $NaNO_3$ as background electrolyte. Solutions of $[Co(tn)_2O_3POC_6H_4NO_2]ClO_4$ were prepared freshly for each kinetic determination by dissolving the complex in ~1 mL of Me_2SO which was then diluted with water, or in a large volume of water directly to give a 2×10^{-4} M solution. Within 30 min an aliquot of this solution was mixed with an equal volume of buffer containing the background electrolyte. The $NaClO_4$ and $NaNO_3$ backgrounds gave kinetic results which were indistinguishable, except that at pH < 10 the experiments using $NaClO_4$ required the presence of a trace of Me_2SO to prevent the precipitation of the reactant.

The following buffers were used (0.025 M buffer and $\mu = 0.50$): pH 6.33, γ-collidine; 7.54, Tris; 8.56, Tris; 9.61, diethanolamine; 10.16, 10.93, and 11.40, triethylamine. For Tris, increasing the buffer concentration to 0.050 M had no observable effect on the rates. For high pH aqueous sodium hydroxide was used, with concentrations in the reaction solutions of 5.00×10^{-3} M, 5.00×10^{-2} M, and 0.500 M.

Generation of *p*-nitrophenol was followed in most cases by spectral measurements at 398 nm. At this wavelength ϵ for *p*-nitrophenolate was 18 700 for 10^{-4} M solutions in 0.50 M $NaClO_4$, at pH 10.93 and 9.61. The apparent ϵ values were also measured for pH 8.56 (18 200) and 7.54 (14 400) to determine the concentrations of released *p*-nitrophenol at these values. For kinetic measurements at pH 6.33 (0.025 M γ-collidine buffer) aliquots of reaction solution were mixed with 0.100 M Tris buffer of pH 8.5 to determine the released *p*-nitrophenol. At 398 nm, in comparison to *p*-nitrophenolate, the absorbancy coefficients of the reactant complex and other products are small. The specific values of ϵ for these species are required for establishing the yields of *p*-nitrophenol. A small correction for the cobalt(III) residue ($[Co(tn)_2PO_4]^0$ (ϵ 73) or $[Co(tn)_2(OH)_2]^+$ (ϵ 54)) amounting to only ~1% of the total change in absorbance was applied.

Pseudo-first-order rate plots (log $(A_\infty - A_t)$ vs. t) were linear to at least 3 half-lives. For the purpose of obtaining rate constants, as well as yields, the values of A_∞ were usually taken after the reaction had proceeded for 8 half-lives. A further very slow production of *p*-nitrophenolate was observed for most solutions, but increases in the absorbance over the next several half-lives amounted to not more than 2% of the total *p*-nitrophenol released, and had no significant bearing on the values of the rate constants for the much faster pseudo-first-order process.

Structural Analysis of $[Co(en)_2PO_4]$. Bis(ethylenediamine)phosphatocobalt(III) crystallizes from water as mauve-red diamond shaped plates. All diffraction measurements were made on crystals mounted with the longest body diagonal set parallel to the goniometer rotation axis. Preliminary precession and Weissenberg photographs showed the crystals to be triclinic, $P1$ or $P\bar{1}$, with the centric space-group ($P\bar{1}$) confirmed by subsequent solution and refinement of the structure. The measured crystal density ($d_m = 1.76$ g cm^{-3}, flotation in aqueous $ZnBr_2$) requires four cobalt phosphate molecules and ten waters of crystallization in the primitive unit cell ($d_c = 1.74$ g cm^{-3}). Precise cell dimensions and the diffractometer orientation matrix were obtained by least-squares refinement of the diffractometer centered setting angles of 12 high angle reflections.[11] Crystal data:[12] $CoPC_4N_4O_4H_{16} \cdot 2.5\ H_2O$, mol wt 318.9 daltons, space group $P\bar{1}$, a = 12.207 (1) Å, b = 9.182 (1) Å, c = 12.038 (1) Å, α = 64.205 (8), β = 89.117 (8), γ = 88.947 (9)°, V = 1214.6 Å^3, $d_m = 1.76$ g cm^{-3}, $Z = 4$, $d_c = 1.74$ g cm^{-3}, λ(Cu Kα_1) = 1.54051 Å, μ(Cu Kα) = 123.4 cm^{-1}, $F(000)$ = 668 e.

Cell dimensions and all reflection data were collected from a crystal with approximate dimensions measured along the crystal edges ([$\bar{1}$01], [101], and [011], respectively) of 0.028 × 0.023 × 0.005 cm. Data (4400) were collected (reflection forms $+h, \pm k, \pm l$; $3 < 2\theta < 125°$) on an automated four-circle diffractometer with graphite-monochromated (monochromator $2\theta = 26.50°$) Cu Kα radiation, a tube takeoff angle of 3.5°, and at a constant temperature of 20 ± 1 °C. Each reflection was scanned using the θ-2θ technique (scan rate 2°/min) from 1° below the calculated Cu Kα_1 position to 1° beyond that of the Cu Kα_2 maximum. Backgrounds were counted for 10 s at either end of the scan range. Three reflections (0,0,−8; 0,7,7; 10,0,0) were measured every 40 data as a check on crystal deterioration and instrument instability. A steady time-dependent decay averaging 18% over the period of the data collection was noted. This was corrected for by applying scale factors, calculated by least squares from the standard reflection intensities, to each batch of 40 data. Lorentz, polarization, and absorption[13] corrections were applied and after merging a set of 3046 unique data with $I \geq 3\sigma(I)$[14] was obtained.[15]

The cobalt and phosphorus atoms were all located from an unsharpened Patterson synthesis and the remaining nonhydrogens found in the succeeding heavy atom phased maps. The structure was refined anisotropically by least squares in two large blocks. The first contained all the parameters of the two independent $[Co(en)_2PO_4]$ molecules and the second the coordinates and temperature factors of the five

Table I. Hydrolysis of *p*-Nitrophenylphosphate Promoted by *trans*-$[Co(tn)_2(OH)(OH_2)]^{2+}$.

[Co complex] × 10^4, M	[PNPP] × 10^4, M[a]	pH	Buffer	μ	$k \times 10^4$, s^{-1} [b]
25.0	1.00	6.7	self-buffered	0.015	0.97
50.0	1.00	6.7	self-buffered	0.015	0.91
50.0	2.00	7.54	Tris[c]	0.036	1.69
50.0	2.00	7.54	Tris[c]	0.50	1.21
50.0	1.00	7.54	Tris[c]	0.50	1.18
50.0	1.00	8.56	Tris[c]	0.50	0.50
50.0	1.00	9.61	Diethanolamine[c]	0.50	0.10

[a] PNPP = *p*-nitrophenylphosphate (disodium salt). [b] 25.0 °C. [c] 0.025 M.

Table II. Stoichiometry for $[Co(tn)_2PO_3OC_6H_4NO_2]ClO_4$ Hydrolysis in NaOH Solutions, 25 °C[a]

NaOH, M	Quenching time, s	$xt_{1/2}$	*p*-Nitrophenol,[b] %	PNPP[c] uncoordinated, %	PNPP[d] on Co(III), %
0.005	23	4	35	28	37
0.005	1.20	20	38	38	24
0.005	900	160	39	54	7
0.01[e]	30	10	41 (42)	30 (44)	29 (14)

[a] Ionic strength 5.1×10^{-3} M. [b] Equal to *p*-nitrophenolate produced after indicated number of $t_{1/2}$. [c] PNPP, *p*-nitrophenylphosphate recovered. [d] Retained on the column and calculated by difference (100% minus sum of columns 3 and 4, total recovery 97%). [e] Values measured from the separations carried out by ion exchange, total recovery 83 ± 1%. Values in parentheses obtained under different elution conditions; see Experimental Section.

independent water oxygens. The scattering factors used were those compiled by Cromer and Waber[16] with the anomalous dispersion corrections for cobalt and phosphorus as given by Cromer.[17] The quantity minimized was $\Sigma w(|F_o| - |F_c|)^2$ where the weight $w = [\sigma(F_o)]^{-2}$.[18] Upon convergence of the refinement, hydrogen atoms[19] were added into the structure factor calculation with isotropic temperature factors set at 1.1 times that of the equivalent *B* value of the parent atom. Hydrogens attached to the $Co(en)_2PO_4$ molecules were placed by calculation (C-H = 0.95 Å, N-H = 0.87 Å)[20] and those on the waters were positioned from peaks found at reasonable locations in the difference maps. Refinement of the nonhydrogen parameters was continued and the hydrogen locating procedures repeated when the calculated shifts became insignificant. A final two cycles of refinement gave $R_1 = \Sigma(||F_o| - |F_c||)/\Sigma|F_o| = 0.063$, $R_2 = [\Sigma w(|F_o| - |F_c|)^2/\Sigma w|F_o|^2]^{1/2} = 0.100$ and the estimated standard error in an observation of unit weight $(=[\Sigma w(|F_o| - |F_c|)^2/(\text{observations} - \text{parameters})]^{1/2})$ of 1.29 for the 3046 observed data. All parameters had shifts less than 0.5 times their esd and inspection of the weighting scheme analysis showed no systematic error dependence on either F_o or $(\sin\theta)/\lambda$. The final difference map showed no peaks greater than 0.75 e $Å^{-3}$, the largest of which were all associated with the heavy atoms.

Results

Hydrolysis Promoted by *trans*-$[Co(tn)_2(OH)(OH_2)]^{2+}$. Preliminary experiments demonstrated that hydrolysis of $Na_2O_3POC_6H_4NO_2$ was greatly enhanced by the *trans*-hydroxo aqua complex. The kinetics of hydrolysis for these conditions with excess complex were followed spectrally (398 nm) at pH 7.54, 8.56, and 9.61. First-order rate constants for the production of *p*-nitrophenolate (>95%) (Table I) are essentially independent of the complex and the nitrophenylphosphate ion over the concentration range used. These results indicate that the hydrolysis rate is not dependent on the rate of coordination of the ligand to the complex ion. However the decrease in the rate of hydrolysis with increasing pH indicates that the rate of entry of the phosphate ester is inhibited by the shift from the hydroxo aqua complex to the dihydroxo species.

Stoichiometry of Hydrolysis of $[Co(tn)_2(O_3POC_6H_4NO_2)]ClO_4$. Total *p*-nitrophenylphosphate in the initial complex was analyzed independently of the microanalytical data by hydrolyzing the *p*-nitrophenolate ion (7%) from the complex and the nitrophenylphosphate ion from the cobalt center in 2 M NaOH. Hydrolysis of nitrophenol from the phosphate residue in acid conditions accounted for 90% of the total amount of *p*-nitrophenol, so that total recovery was 97%.

Some experiments also detected *p*-nitrophenylphosphate coordinated to the cobalt center after the initial hydrolysis of *p*-nitrophenolate ion was complete. Freshly dissolved $[Co(tn)_2(O_3POC_6H_4NO_2)]ClO_4$ (2×10^{-4} M) was treated with an equal volume of NaOH solution (0.0100 M). In separate experiments these solutions were quenched with HCl (to pH ~ 3) after 23, 120, and 900 s (corresponding to 4, 20, and 160 $t_{1/2}$ for hydrolysis to *p*-nitrophenolate ion at this ionic strength). An aliquot of each quenched solution was used to determine the yield of *p*-nitrophenolate ion and the bulk of each quenched solution was adsorbed on a cation exchange resin (H^+ form) which was then eluted with dilute $HClO_4$ (pH ~ 3). The effluent solution and washings were sampled for *p*-nitrophenolate before hydrolysis of any *p*-nitrophenylphosphate (in 1 M HCl at 100 °C for 4 h). The solutions were made alkaline with NaOH and the *p*-nitrophenolate determined spectrophotometrically. The results for these experiments are given in Table II.

Approximately 65% of the nitrophenyl residue remained bound to the phosphate after the initial hydrolysis. Of this 37% was attached to cobalt after $4t_{1/2}$ for the hydrolysis reaction and this fraction was captured on the cation exchange column. The remaining 28% passed through as *p*-nitrophenylphosphate. After longer periods more of the *p*-nitrophenylphosphate was cleaved from the cobalt residue and after $160t_{1/2}$ only 7% of the phosphate ester remained attached to cobalt.

The attachment of a portion (37–41%) of the *p*-nitrophenylphosphate to the cobalt ion was proved by adsorbing the reaction mixture on a cation exchange column and eluting with 0.1–0.2 M in $NaClO_4$. Released *p*-nitrophenol and *p*-nitrophenylphosphate were monitored. In an independent experiment $[Co(tn)_2PO_4]$ was retained on the ion-exchange resin presumably through ring opening and protonation to produce a cation and it therefore contaminates band 1 or 2. The results are shown in Table II (row 4) and it is seen that they differ except for the amount of *p*-nitrophenol produced. The differences come from the times used to elute the complexed *p*-nitrophenylphosphate and the details are given in the Experimental Section. It is clear that some hydrolysis of the mono-

Table III. Yields and Rate Constants for Production of *p*-Nitrophenyl from $[Co(tn)_2(O_3POC_6H_4NO_2)]^+$ in Aqueous Solution

pH	Buffer	k, s^{-1} [b]	k_{OH}, $M^{-1}s^{-1}$	Yield,[c] %
6.33	γ-Collidine[d]	8.4×10^{-5}		36
7.54	Tris[d]	1.02×10^{-4}		30
8.56	Tris[d]	1.33×10^{-4}		33
9.61	Diethanolamine[d]	4.54×10^{-4}		37
10.16	Triethylamine	1.72×10^{-3}		36
10.93	Triethylamine	8.02×10^{-3}		40
11.40	Triethylamine	2.11×10^{-2}		40
11.53[e]	5.0×10^{-3} M NaOH	2.56×10^{-2}	5.1	39
12.53[e]	5.0×10^{-2} M NaOH	2.39×10^{-1}	4.8	33
13.53[e]	0.50 M NaOH	2.64	5.3	14
	0.50 M NaOH	0.99[f]		
	2.00 M NaOH			7
	5.0×10^{-3} M NaOH	0.12[g]		

[a] 25.0 °C; ionic strength = 0.50, except for last three entries; initial concentration of $[Co(tn)_2PO_3OC_6H_4NO_2]^+ \sim 10^{-4}$ M. [b] Each entry is average of at least two values which differ by not more than 10%. [c] Yield (%) = percentage of complex hydrolyzed to *p*-nitrophenol(ate) after 8 half-lives for first-order process. [d] 0.025 m. [e] pH taken as $-\log_{10} a_{H^+}$ with an activity coefficient of 0.68 s. J. F. Kirsch and W. P. Jencks, *J. Am. Chem. Soc.*, **86**, 837 (1964). [f] Ionic strength 1.0 m.

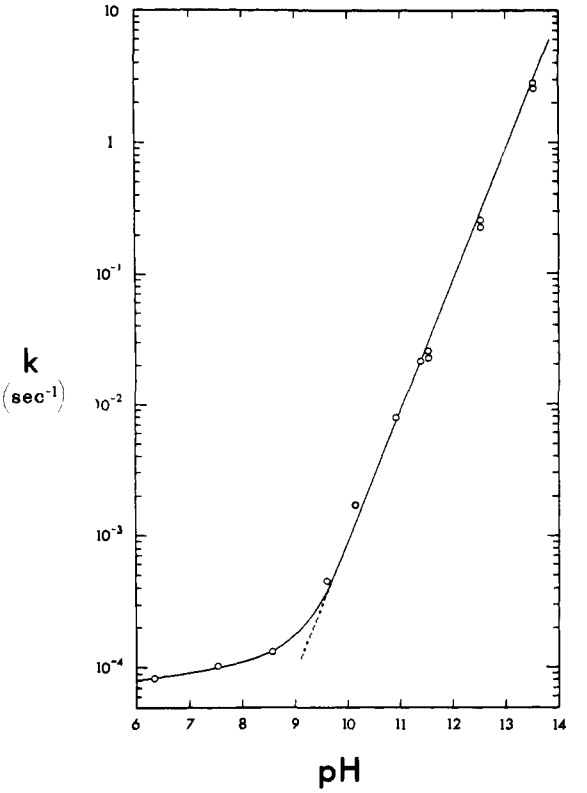

Figure 1. pH dependence of the rate constant (at 25 °C) for production of *p*-nitrophenol from $[Co(tn)_2(O_3POC_6H_4NO_2)]^+$.

dentate *p*-nitrophenylphosphate to *p*-nitrophenol occurs during this elution process.

Hydrolysis of $[Co(tn)_2O_3POC_6H_4NO_2]ClO_4$. The hydrolysis of *p*-nitrophenol(ate) from the complex was followed spectrophotometrically near 400 nm from pH 6 to 13.5 at 25 °C. A pseudo-first-order process for the production of *p*-nitrophenol(ate) was observed with yields ~35% except at pH > 13 where the yield of *p*-nitrophenolate ion decreased as the OH^- concentration increased. This rapid reaction was followed by a much slower process (>100-fold) which also released *p*-nitrophenolate ion, but which did not complicate the observation of the kinetics for the initial burst of *p*-nitrophenol(ate). The results of the kinetic study are given in Table III and Figure 1.

The data indicate a first-order dependence of the initial hydrolysis on the OH^- concentration in the basic region, approaching a limiting rate in neutral to slightly acid conditions such that:

$$k_{obsd} = k_{H_2O} + k_{OH^-}[OH^-]$$

where $k_{H_2O} = 7 \times 10^{-5}\ s^{-1}$ and $k_{OH^-} = 5.1\ M^{-1}\ s^{-1}$ based on the OH^- concentration. The rate constants were independent of the buffer or the buffer concentration.

The hydrolysis was also followed crudely by ^1H NMR spectroscopy in dimethyl-d_6 sulfoxide-D_2O mixtures (2:1 by volume). Limited solubility of the complex precluded use of D_2O as the sole solvent. Some results of the NMR study are shown in Figure 2. The signals displayed are for the aromatic protons and the chemical shifts and coupling constants coincide with the conversion of chelated *p*-nitrophenylphosphate to free nitrophenol. The half-life under these conditions is ~1 day ($k \sim 8 \times 10^{-6}\ s^{-1}$) and the reactions proceed with the development of the yellow color due to *p*-nitrophenolate ion.

In the mixed solvent with the complex at the high concentration needed for detection of NMR the hydrolysis proceeds essentially to completion (~90%). Presumably this arises from recombination of *p*-nitrophenylphosphate ion and $[Co(tn)_2(OH)(OH_2)]^{2+}$, a process which is minimized in the more dilute spectrophotometric reaction mixtures.

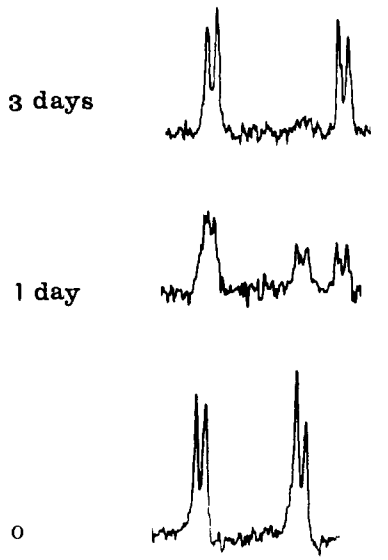

Figure 2. The change in aromatic proton resonances during hydrolysis of $[Co(tn)_2(O_3POC_6H_4NO_2)]^+$.

^{18}O Tracer Study. The hydrolysis of $[Co(tn)_2(O_3POC_6H_4NO_2)]^+$ ion in 0.1 M NaOH containing 4.586 atom % $H_2{}^{18}O$ showed that the barium nitrophenylphosphate salt, which was isolated, contained little of the isotopic enrichment of the solvent, 0.261 atom % $H_2{}^{18}O$. The small enrichment observed over the normal isotopic enrichment of ^{18}O (0.201 atom %) may be attributed to a small amount of $Ba_3(PO_4)_2$ arising from the abstraction of PO_4^{3-} ion by Ba^{2+} from the $[Co(tn)_2PO_4]$ complex or residual $^{18}OH_2$ in the lattice. Blank experiments showed that solutions of Ba^{2+} and $[Co(tn)_2PO_4]$ slowly deposit the barium phosphate as a gelatinous mass.

Table IV. Final Atomic Parameters with Their Esd's for Phosphatobis(ethylenediamine)cobalt(III)[a]

ATOM	X/A	Y/B	Z/C	BETA11	BETA22	BETA33	BETA12	BETA13	BETA23
CO(1)	0.5748(1)	0.2087(1)	0.3031(1)	0.0041(1)	0.0092(1)	0.0040(1)	0.0004(1)	0.0009(1)	-0.0013(1)
P(1)	0.7412(1)	0.0664(2)	0.4329(1)	0.0042(1)	0.0045(2)	0.0029(1)	0.0004(1)	0.0004(1)	-0.0006(1)
O(11)	0.6257(3)	0.1030(5)	0.4728(3)	0.0030(3)	0.0084(6)	0.0027(3)	-0.0003(4)	0.0011(3)	-0.0004(4)
O(12)	0.7236(3)	0.1444(5)	0.2893(3)	0.0034(3)	0.0098(7)	0.0026(3)	0.0011(4)	0.0012(3)	-0.0006(4)
O(13)	0.7632(4)	-0.1138(5)	0.4860(4)	0.0083(5)	0.0053(6)	0.0038(4)	0.0009(4)	-0.0001(3)	-0.0010(4)
O(14)	0.8314(3)	0.1509(5)	0.4658(4)	0.0023(3)	0.0109(7)	0.0069(4)	-0.0018(4)	0.0004(3)	-0.0055(5)
N(11)	0.4323(4)	0.2702(6)	0.3457(4)	0.0041(4)	0.0078(8)	0.0033(4)	-0.0002(5)	0.0011(3)	-0.0004(5)
N(12)	0.6236(4)	0.4161(6)	0.2888(4)	0.0026(4)	0.0086(8)	0.0038(4)	-0.0002(4)	0.0006(3)	-0.0011(5)
N(13)	0.5437(4)	0.2997(6)	0.1282(4)	0.0033(4)	0.0103(9)	0.0035(4)	0.0014(5)	0.0008(3)	-0.0011(5)
N(14)	0.5217(4)	0.2094(6)	0.3133(4)	0.0036(4)	0.0063(7)	0.0042(4)	0.0007(4)	0.0007(3)	-0.0008(5)
C(11)	0.4502(6)	0.3943(8)	0.3892(6)	0.0049(6)	0.0096(10)	0.0052(6)	0.0009(6)	0.0017(5)	-0.0032(6)
C(12)	0.5292(6)	0.5149(7)	0.2983(6)	0.0048(6)	0.0056(9)	0.0068(6)	-0.0005(6)	0.0019(5)	-0.0026(6)
C(13)	0.5309(6)	0.1629(8)	0.0931(6)	0.0071(7)	0.0128(11)	0.0035(5)	0.0004(7)	0.0007(5)	-0.0029(6)
C(14)	0.4653(6)	0.0325(8)	0.1974(6)	0.0055(6)	0.0098(10)	0.0060(6)	0.0005(6)	-0.0006(5)	-0.0035(7)
CO(2)	0.0683(1)	0.2952(1)	0.2001(1)	0.0040(1)	0.0090(1)	0.0037(1)	0.0002(1)	0.0008(1)	-0.0014(1)
P(2)	0.2398(1)	0.4044(2)	0.0663(1)	0.0024(1)	0.0051(2)	0.0019(1)	0.0001(1)	0.0009(1)	-0.0005(1)
O(21)	0.1258(3)	0.4889(4)	0.0650(3)	0.0021(3)	0.0065(6)	0.0037(3)	0.0011(3)	0.0004(3)	-0.0003(4)
O(22)	0.2134(3)	0.2296(4)	0.1699(3)	0.0035(3)	0.0047(6)	0.0027(3)	0.0007(3)	0.0007(3)	0.0007(3)
O(23)	0.3317(3)	0.4795(5)	0.1061(4)	0.0022(3)	0.0088(7)	0.0067(4)	-0.0014(4)	-0.0006(3)	-0.0042(4)
O(24)	0.2696(4)	0.4033(5)	-0.0557(4)	0.0078(5)	0.0087(7)	0.0028(4)	-0.0002(4)	0.0021(3)	-0.0017(4)
N(21)	-0.0068(4)	0.3996(6)	0.2124(4)	0.0038(4)	0.0074(8)	0.0033(4)	0.0003(5)	0.0003(3)	-0.0005(5)
N(22)	0.1259(4)	0.3655(6)	0.3193(4)	0.0031(4)	0.0073(7)	0.0034(4)	-0.0012(4)	0.0006(3)	-0.0012(4)
N(23)	0.0281(4)	0.0846(6)	0.3298(4)	0.0036(4)	0.0075(8)	0.0028(4)	0.0004(4)	0.0005(3)	-0.0003(4)
N(24)	0.0042(4)	0.2214(6)	0.0857(4)	0.0039(4)	0.0088(8)	0.0031(4)	0.0004(5)	0.0002(3)	-0.0014(5)
C(21)	-0.0457(6)	0.5122(8)	0.2667(6)	0.0045(6)	0.0123(11)	0.0055(6)	0.0022(6)	0.0008(5)	-0.0038(7)
C(22)	0.0339(6)	0.4261(8)	0.3716(6)	0.0052(6)	0.0119(11)	0.0041(5)	0.0003(6)	0.0010(4)	-0.0040(6)
C(23)	0.0004(6)	-0.0259(7)	0.2738(6)	0.0056(6)	0.0068(9)	0.0052(6)	-0.0007(6)	0.0013(5)	-0.0014(6)
C(24)	-0.0696(6)	0.0736(8)	0.1553(6)	0.0045(6)	0.0136(12)	0.0051(6)	-0.0011(6)	0.0012(4)	-0.0046(7)
OX(1)	-0.2535(6)	0.7058(7)	0.3677(5)	0.0180(9)	0.0155(10)	0.0095(6)	-0.0028(8)	0.0014(6)	-0.0077(7)
OX(2)	0.1970(5)	0.9933(6)	0.0769(5)	0.0092(5)	0.0137(9)	0.0103(6)	-0.0008(6)	0.0020(4)	-0.0067(6)
OX(3)	0.2687(5)	0.6802(6)	0.2158(5)	0.0116(6)	0.0146(9)	0.0085(6)	0.0000(6)	0.0013(5)	-0.0052(6)
OX(4)	0.2383(5)	0.6162(6)	0.4658(5)	0.0130(7)	0.0122(9)	0.0095(6)	0.0024(6)	-0.0004(5)	-0.0062(6)
OX(5)	0.6877(6)	0.8326(6)	0.1288(5)	0.0148(7)	0.0128(9)	0.0096(6)	0.0011(7)	0.0014(5)	-0.0052(6)

ATOM	X/A	Y/B	Z/C	B(A**2)	ATOM	X/A	Y/B	Z/C	B(A**2)
H(11)	0.479	0.346	0.469	3.2	H(21)	0.390	0.307	0.281	2.5
H(12)	0.381	0.446	0.390	3.2	H(22)	0.401	0.184	0.404	2.5
H(13)	0.496	0.575	0.219	2.8	H(23)	0.669	0.399	0.347	2.4
H(14)	0.553	0.590	0.328	2.8	H(24)	0.655	0.466	0.217	2.4
H(15)	0.598	0.521	0.282	3.3	H(25)	0.485	0.358	0.111	2.6
H(16)	0.489	0.599	0.218	3.3	H(26)	0.599	0.358	0.085	2.6
H(17)	0.391	0.465	0.201	3.4	H(27)	0.578	-0.060	0.322	2.2
H(18)	0.464	-0.068	0.189	3.4	H(28)	0.477	-0.038	0.375	2.2
H(19)	-0.111	0.539	0.298	2.9	H(29)	-0.097	0.450	0.141	2.5
H(110)	-0.070	0.609	0.205	2.9	H(210)	-0.114	0.325	0.261	2.5
H(111)	0.064	0.502	0.398	2.9	H(211)	0.157	0.284	0.379	2.0
H(112)	0.011	0.341	0.437	2.9	H(212)	0.173	0.441	0.283	2.0
H(113)	-0.045	-0.110	0.328	3.1	H(213)	0.084	0.247	0.379	2.5
H(114)	0.065	-0.071	0.256	3.1	H(214)	-0.027	0.299	0.371	2.5
H(115)	-0.066	0.012	0.109	3.4	H(215)	-0.040	0.296	0.334	2.2
H(116)	-0.131	0.101	0.174	3.4	H(216)	0.056	0.200	0.243	2.2
HO(11)	-0.259	0.762	0.391	6.0	HO(32)	0.327	0.175	0.182	5.3
HO(12)	-0.253	0.606	0.406	6.0	HO(41)	0.199	0.682	0.468	4.8
HO(21)	0.242	1.026	0.118	4.5	HO(42)	0.247	0.664	0.393	4.8
HO(22)	0.25	1.061	0.0	4.5	HO(51)	0.713	0.788	0.231	5.6
HO(31)	0.238	0.780	0.155	5.3	HO(52)	0.7	0.727	0.100	5.6

[a] The form of the anisotropic temperature parameter is $\exp[-(\beta_{11}h^2 + \beta_{22}k^2 + \beta_{33}l^2 + 2\beta_{12}hk + 2\beta_{13}hl + 2\beta_{23}kl)]$.

Description of the $[Co(en)_2PO_4]$ Structure. The final refined atom parameters are given in Table IV. Figure 3 is a perspective view of the two independent $[Co^{III}(en)_2PO_4]$ molecules contained in one crystallographic asymmetric unit. The structures shown here have the Δ-(λλ)- and Λ-(δδ)- conformations, although in the crystal the mirror images of both molecules also occur. Molecule 1 is thus present with the conformations Δ-(λλ) and Λ-(δδ)- as is molecule 2. Equivalent bond lengths and angles (Table V) show few significant differences and the few exceptions are probably due to the nonequivalent crystal environments. The ethylenediamine chelate rings have dimensions similar to those found for other $Co^{III}(en)$ complexes.[21-24] The Co-N distances vary between 1.939 and 1.958 Å (3σ) while the in-ring angles at the cobalt are all close to 86°. Torsion angles are listed in Table VI.

Figure 4 shows the mean bond lengths and angles for the coordinated phosphate ring. The Co-P distance for molecule 1 is 2.549 (2) Å, while that for the second molecule is 2.559 (2) Å. The atoms of the four-membered ring in molecule 1 do not significantly deviate from the mean plane[25] $0.3405X + 0.9373Y - 0.0741Z - 5.4604 = 0$, although in molecule 2 both oxygens lie about 0.038 Å above the best plane $-0.3787X - 0.6343Y - 0.6740Z + 4.1918 = 0$. The phosphorus P(2) thus lies 0.067 Å above the O-Co-O plane (toward O(23)) and probably reflects the differences in the hydrogen bonding of the two phosphates.

Table V. Bond Lengths and Angles for $[Co(en)_2PO_4]\cdot 2.5H_2O$

	Molecule 1	Molecule 2
	A. Bond Lengths	
Co-N(1)	1.948 (6)[a]	1.941 (6)
Co-N(2)	1.939 (6)	1.953 (6)
Co-N(3)	1.939 (5)	1.951 (4)
Co-N(4)	1.951 (7)	1.958 (6)
Co-O(1)	1.948 (4)	1.948 (3)
Co-O(2)	1.927 (4)	1.940 (4)
Co-P	2.549 (2)	2.559 (2)
P-O(1)	1.560 (5)	1.578 (4)
P-O(2)	1.574 (4)	1.581 (3)
P-O(3)	1.510 (5)	1.515 (5)
P-O(4)	1.513 (4)	1.499 (5)
N(1)-C(1)	1.467 (10)	1.474 (11)
C(1)-C(2)	1.519 (9)	1.519 (9)
C(2)-N(2)	1.487 (9)	1.488 (9)
N(3)-C(3)	1.500 (11)	1.488 (10)
C(3)-C(4)	1.532 (9)	1.516 (9)
C(4)-N(4)	1.482 (9)	1.483 (8)
	B. Bond Angles	
N(1)-Co-N(2)	85.6 (2)	85.9 (2)
N(1)-Co-N(3)	93.9 (2)	94.1 (2)
N(1)-Co-N(4)	93.2 (2)	91.9 (2)
N(1)-Co-O(1)	94.6 (2)	94.0 (2)
N(1)-Co-O(2)	169.8 (2)	169.8 (2)
N(2)-Co-N(3)	91.6 (2)	92.1 (2)
N(2)-Co-N(4)	178.0 (2)	177.0 (2)
N(2)-Co-O(1)	90.5 (2)	90.2 (2)
N(2)-Co-O(2)	90.9 (2)	91.6 (2)
N(3)-Co-N(4)	86.8 (2)	86.0 (2)
N(3)-Co-O(1)	171.4 (2)	171.7 (2)
N(3)-Co-O(2)	95.8 (2)	95.9 (2)
N(4)-Co-O(1)	91.2 (2)	92.0 (2)
N(4)-Co-O(2)	90.5 (2)	90.9 (2)
O(1)-Co-O(2)	75.8 (2)	76.1 (2)
O(1)-P-O(2)	98.8 (2)	98.6 (2)
O(1)-P-O(3)	112.3 (3)	111.9 (3)
O(1)-P-O(4)	111.0 (2)	111.5 (2)
O(2)-P-O(3)	110.8 (2)	110.8 (2)
O(2)-P-O(4)	112.3 (3)	112.0 (3)
O(3)-P-O(4)	111.1 (3)	111.5 (3)
Co-N(1)-C(1)	107.7 (4)	109.0 (4)
N(1)-C(1)-C(2)	106.6 (6)	106.8 (6)
C(1)-C(2)-N(2)	105.3 (5)	106.1 (6)
C(2)-N(2)-Co	110.8 (4)	109.8 (4)
Co-N(3)-C(3)	108.2 (3)	109.5 (3)
N(3)-C(3)-C(4)	106.6 (6)	107.3 (5)
C(3)-C(4)-N(4)	106.0 (6)	107.0 (6)
C(4)-N(4)-Co	109.7 (4)	109.9 (4)
Co-O(1)-P	92.5 (2)	92.5 (2)
Co-O(2)-P	92.9 (2)	92.7 (2)

[a] The numbers in parentheses are the estimated standard deviations in the least significant digits given.

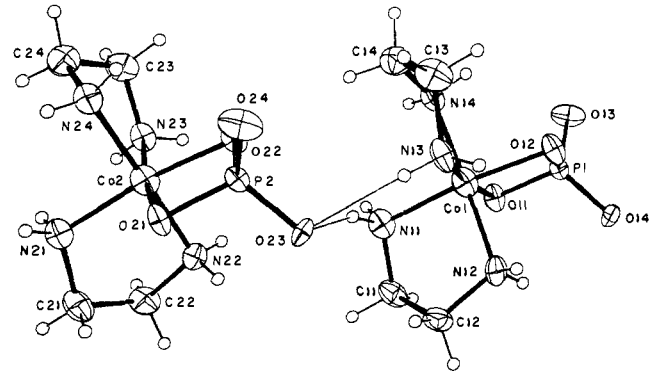

Figure 3. Perspective view of the two crystallographically independent molecules of $[(en)_2CoPO_4]$. Fine lines indicate hydrogen bonding between molecules 1 and 2.

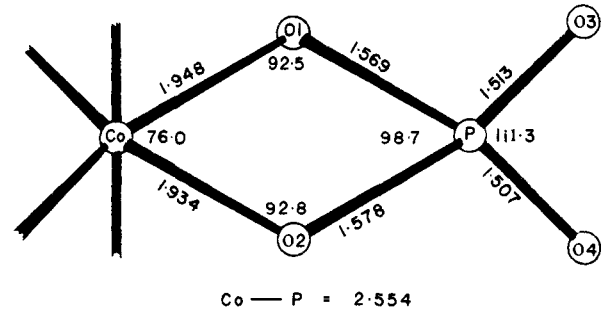

Figure 4. Mean geometry of the phosphato-cobalt(III) chelate ring.

Table VI. Torsion Angles for $[Co(en)_2PO_4]\cdot 2.5H_2O$

	Molecule 1	Molecule 2
Co-N(1)-C(1)-C(2)	45.8 (5)	−42.2 (5)
N(1)-C(1)-C(2)-N(2)	−52.0 (7)	50.9 (6)
C(1)-C(2)-N(2)-Co	34.5 (6)	−36.4 (6)
Co-N(3)-C(3)-C(4)	41.1 (6)	−38.2 (6)
N(3)-C(3)-C(4)-N(4)	−51.2 (7)	48.8 (7)
C(3)-C(4)-N(4)-Co	37.7 (7)	−37.2 (7)

The chelate angle O(1)-Co-O(2) has a mean value of 76.0 (2)°, which is somewhat larger than the values of 68.8[26] and 69.3° [27] found for the four-membered carbonato chelate rings, but is much less than the normal octahedral geometry preferred by cobalt(III). The less strained six-membered ring of $[Co(en)_2HP_2O_7]$[24] has an O-Co-O angle of 92.8 (2)°. The two Co-O bonds (mean, 1.948, 1.933) are similar to those found in the pyrophosphate complex[24] and other Co-oxyanion structures.[26,28] No correlation between bond length and strain is evident.

The in-ring O-P-O angle has been deformed from the unstrained tetrahedral value to 98.7 (2)° similar in magnitude to that found in methylethylenephosphate[29] (99.1 (6)°) and cytidine 2′,3′-cyclic phosphate (95.8 (4)°),[30] while the adjacent bonds (mean, 1.573 (4) Å) are more similar to methylethylenephosphate (1.57 (1) Å)[29] and the unstrained values found in arginine diethylphosphate[31] (mean, 1.58 (1) Å), magnesium diethylphosphate[32] (1.563 (6) Å), and ammonium dimethylphosphate (1.559 (7) Å)[33] than the more highly constrained cyclic phosphate (1.613 (4) Å)[30]. The two monovalent oxygens form bonds with the phosphorus of 1.513 (5) and 1.507 (5) Å, respectively, and all O-P-O angles apart from the endocyclic one are only slightly larger than the tetrahedral value, ranging between 110.8 and 112.3°. This can be contrasted with the ionic disubstituted phosphates[30,33] where the equivalent bonds are all shorter (1.44-1.428 Å) and the O(3)-P-O(4) angle is invariably widened to about 117°.

The arrangement of the individual molecules within the crystal is shown in Figure 5 and a list of all intermolecular approaches <3.2 Å is given in Table VII. The crystal is composed of discrete Δ-(λλ)- (molecule 1) and Λ-(δδ)- (molecule 2) units alternating along chains approximately parallel to *a* together with the antiparallel chains of enantiomers. Molecule 2 has rotated from the orientation of molecule 1 by about 48° and is bound to it by the hydrogen bonds O(23)-N(11) (2.953 Å) and O(23)-N(13) (2.966 Å), while O(13) can be considered connected to the next molecule 2 by weak hydrogen bonds to N(21) (3.155 Å) and N(23)(3.083 Å). The antiparallel chains are held together by a number of hydrogen bonds which vary in length between 2.820 and 3.154 Å to bind the whole into a solid framework. In addition the five water molecules

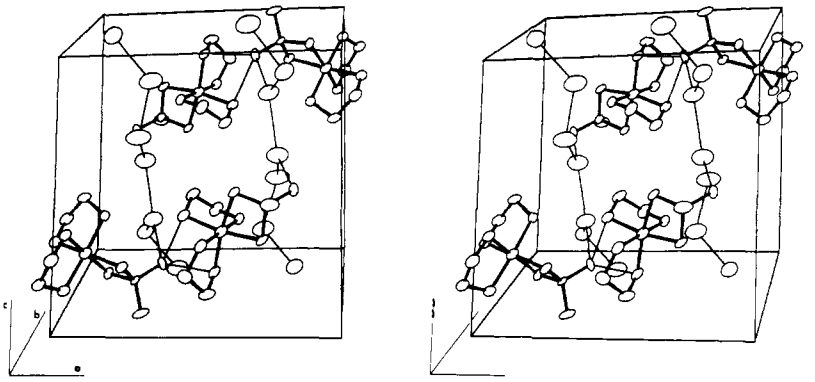

Figure 5. Stereoview of the unit cell contents of $[(en)_2CoPO_4]\cdot 2.5H_2O$. Fine lines represent some of the hydrogen bonding which is present.

Table VII. Intermolecular Contacts (<3.2 Å) in the Crystal Structure of $[Co(en)_2PO_4]\cdot 2.5\ H_2O$

Atoms A	Atoms B	d (A···B), Å	Symmetry operation[a]
N(11)	O(23)	2.953	x, y, z
N(11)	O(14)	3.051	$1-x, -y, 1-z$
N(12)	O(24)	2.899	$1-x, 1-y, -z$
N(13)	O(23)	2.996	x, y, z
N(13)	O(23)	3.063	$1-x, 1-y, -z$
N(14)	O(11)	2.925	$1-x, -y, 1-z$
O(13)	N(21)	3.155	$1+x, y, z$
O(13)	N(23)	3.006	$1-x, -y, 1-z$
O(13)	N(23)	3.083	$1+x, y, z$
O(13)	OX(4)	2.725	$1-x, 1-y, 1-z$
O(14)	N(22)	2.820	$1-x, -y, 1-z$
O(14)	OX(1)	2.625	$1+x, y-y, z$
N(21)	O(21)	3.125	$-x, 1-y, -z$
N(21)	O(24)	3.099	$-x, 1-y, -z$
N(22)	OX(3)	3.153	x, y, z
N(24)	O(21)	2.936	$-x, 1-y, -z$
N(24)	OX(2)	3.154	$x, y-1, z$
O(22)	OX(2)	2.853	$x, y-1, z$
O(23)	OX(3)	2.786	x, y, z
O(24)	OX(5)	2.721	$1-x, 1-y, -z$
OX(1)	OX(4)	2.762	$-x, 1-y, 1-z$
OX(1)	OX(5)	2.694	$x-y, y, z$
OX(2)	OX(3)	2.756	x, y, z
OX(2)	OX(5)	2.684	$1-x, 2-y, -z$
OX(3)	OX(4)	2.824	x, y, z

[a] To move atom B into contact with atom A.

of crystallization lie in a zigzag chain (parallel to the (011) plane) between the antiparallel chains of phosphates binding strongly to each other and to the phosphate oxygens. The O-O distance for these bonds varies between 2.625 and 2.853 Å. Each monovalent phosphate oxygen is bound to one of the waters as is O(22) (O(22)-OX(2), 2.853 Å), although the equivalent O(12) remains free. It may be that it is this additional hydrogen bond which distorts the coordinated phosphate ring of molecule 2 into its observed nonplanarity.

Discussion

The characterization of $[Co(tn)_2(O_3POC_6H_4NO_2)]ClO_4$ as an anhydrous salt along with its behavior as a mononuclear monovalent cation on neutral cation-exchange resins is direct evidence for the phosphate ester being bound as a chelate. This assertion is also supported by the kinetic, tracer, and stoichiometry results. All indicate competitive paths for the hydrolysis reaction; one involving cleavage of *p*-nitrophenol, the other involving cleavage of the chelate ring at one Co-O bond. In addition there is a slower consecutive process which involves the cleavage of the monodentate *p*-nitrophenylphosphate from the Co(III) center. The stereochemistry of the monodentate species was not ascertained, but other studies[8] with bis(trimethylenediamine)cobalt(III) ions indicate that the cis-trans rearrangement should be rapid and should favor the cis configuration. Except for the highly basic conditions both the base independent path and the path first order in OH^- give 35 ± 5% release of *p*-nitrophenol and $[Co(tn)_2PO_4]$. The path first order in OH^- which gives the initial burst of *p*-nitrophenol is interpreted as attack of OH^- at the phosphorus atom of the chelated ester dianion, Figure 6 (path a). Simultaneously ~65% Co-O cleavage occurs and the stoichiometry experiments show that after 4 half-lives for the loss of *p*-nitrophenol, 37% of the total phosphate is still bound to cobalt(III) as the monodentate ester and 28% has been cleaved totally from the Co(III) center as *p*-nitrophenylphosphate. Both of the last reactions are consistent with the conjugate base mechanism (S_N1cB) for hydrolysis of many anion ligands from analogous Co(III) amine complexes, Figure 6, path b. The preliminary step is a preequilibrium deprotonation of a trimethylenediamine-NH_2 group followed by dissociation of one end of the phosphate chelate as a rate-determining process to give a five-coordinate intermediate. Water capture by this intermediate yields the hydroxo or aqua phosphate ester complex. Complete loss of ester from the complex then occurs by the same type of mechanism to give the dihydroxo or hydroxo aqua ion. The ^{18}O trace experiment supports this path over that of ring opening occurring by P-O rupture in the five-coordinate phosphorus intermediate. Clearly the latter should lead to one oxygen enriched in the monodentate ester and at least one in the cleaved ester dianion, whereas only 1.4% of the total ^{18}O label is incorporated.

We considered trying to separate the Co-O, P-O cleavages by varying the temperature, but inspection of relevant data on P ester cleavage and Co-OPO_3 cleavage indicated the activation energies were both in the vicinity of 30 kcal/mol and little discrimination could be expected.

The most significant result observed was the rapid hydrolysis of *p*-nitrophenylphosphate. The extrapolated rate constants for hydrolysis of the free ester and those observed for the chelated ester are given in Table VIII. The greatest difference occurred in the alkaline region where an acceleration ~10^9 was observed for the chelate. The magnitude of this effect can be largely accommodated by the type of strain relief proposed by Westheimer et al.[34] to explain the accelerations observed with methylethylenephosphate and five-membered cyclic phosphonates relative to analogous esters lacking strained rings.

The proposal for the mechanism for the chelated ester hydrolysis is depicted in Figure 6, path a. We presume base attack occurs to generate the five-coordinate phosphorane with OH^- initially in an apical position and that pseudorotation then occurs with $-O^-$ as the pivot group. This introduces OH into an equatorial position and allows *p*-nitrophenol to leave from

Table VIII. Comparison of Rate Constants (s^{-1}) for Hydrolysis of Chelated and Uncoordinated *p*-Nitrophenylphosphate at 25 °C.

pH	PNPP[a,b]	$[Co(tn)_2PNPP]^+$	Rate ratio
7.5	5.7×10^{-9}	1.2×10^{-4}	2×10^4
10.2	1.4×10^{-9}	1.4×10^{-3}	10^6
13.5[c]	2×10^{-9}	2.6	$\sim 10^9$

[a] Extrapolated from the data of A. J. Kirby and W. P. Jencks, *J. Am. Chem. Soc.*, **87**, 3209 (1965). [b] PNPP = *p*-nitrophenylphosphate. [c] 0.50 M NaOH.

an apical site. The mechanism is consistent with the general features of organic phosphorus ester chemistry,[5] but there are some aspects of the behavior of the metal chelate which contrast sharply with the base hydrolysis of methylethylenephosphate. For example, in the pH range 9–14 the latter hydrolyzes almost solely by ring opening.[35] For the inorganic chelate only exocyclic P–O hydrolysis is observed. This result is somewhat surprising, since the four-membered ring should open more readily than the five-membered ring. In part the problem is resolved by Co–O bond rupture occurring in competition with that of P–O. Generally, Co–O cleavage would be expected to be the more facile process in such chelates.[36] For organic phosphates, esters containing five-membered rings are much more reactive than their acyclic counterparts and also their homologues containing six- and seven-membered rings.[37] We can anticipate, therefore, that four-membered cyclic esters will be very reactive and the metal chelate approximates this situation. The present results do not indicate whether reaction may be further facilitated by proton transfer within the phosphorane intermediate, allowing the neutral phenol to be the leaving group, as no general-base catalysis was seen. Proton transfer catalyzed by water would, however, lead to a decomposition pathway without charge separation, which would deliver nitrophenol and the chelated phosphato complex, the thermodynamically favored forms,[38] as the immediate products. Additional rate enhancement due to the metal ion may arise as a consequence of charge neutralization.[4,39] Hydroxide ion should add more readily to the cationic complex than to the dianion of the uncoordinated ester, though some evidence exists that such effects of charge on rate are not large.[40]

The strain in the parent chelate is real enough if the geometry of the chelated ester parallels that observed for the chelated PO_4^{3-} ion. Here the Co–O–P–O ring is essentially planar, Figure 4, the O–Co–O angle is 76° and the O–P–O angle is 98.7°. The preferred angles would be 90 and 109°, respectively, to preserve the octahedral and tetrahedral geometries. The Co–O–P angles are ~103° and the Co–P distance is 2.54 Å, which is extraordinarily short and close to the sum of the covalent radii for Co (1.22 Å) and P (1.10 Å). Usually the Co–Co distance in Co–OH–Co–OH dimers, for example, is ~2.9 Å and the Co–O–Co angle ~90–103°.[41] Widening the O–P–O angle to 108° while keeping the bond lengths constant improves the geometry at the O–Co–O angle relative to the strain free value, but now the Co–O–P angles are more strained (~80°) and the Co–P distance becomes less than the sum of the covalent radii (2.2 Å). The last effect may be an important factor and recent accurate crystallographic studies have shown that in Co(III) complexes containing either NH_3 or CN^- the integrated electron density about Co in a sphere of radius 1.22 Å is 26.3 and 26.7 ± 0.3 e, respectively. This is probably the best evidence for the Pauling electroneutrality principle and provides us with a realistic minimum distance for the approach of another nonbonded atom to Co(III) in this type of molecule. The analysis indicates that the chelated phosphate ring is strained not only by bond angle strain, but also by the proximity of the Co and P atoms. In the five-coordinated P intermediate it is likely that the apical and equatorial P–O bonds

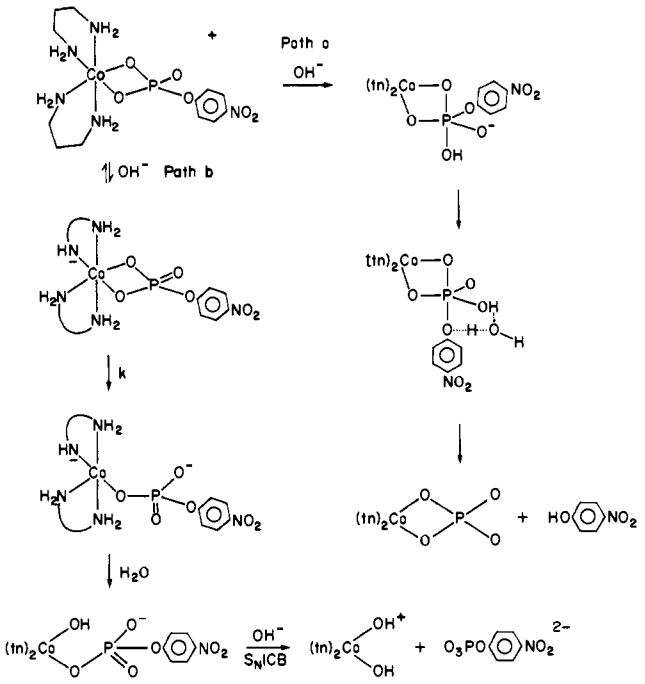

Figure 6. Reaction pathways for the base hydrolysis of $[Co(tn)_2O_3PO\text{-}C_6H_4NO_2]^+$.

will differ and reasonable estimates are 1.75 and 1.63 Å, respectively.[43] Using these bond lengths with the measured Co–O bond lengths, the geometry of the chelate with a 90° O–P–O angle is calculated as Co–O–P angles of 95 and 99° and the O–Co–O angle is unchanged at 76°. The calculated Co–P distance under these circumstances is 2.75 Å, which would relieve the nonbonded interaction between the Co and P atoms. Moreover, the chelate angle subtended at phosphorus is strain free and the strain in the Co–O–P angles has been relieved. Only the O–Co–O angle remains strained to the same degree as the reactant. In short, there is good evidence for strain in the four-membered chelate which would be relieved in a five-coordinate intermediate. Also the O–P–O angle for the chelate is essentially the same as that for the the ethylenephosphate chelate. These effects must contribute to the rate enhancements observed, but it is difficult to quantify them until our knowledge of the force fields and geometries of the five-coordinate P intermediates improves.

The slow secondary hydrolysis after the initial burst of *p*-nitrophenol at high pH is accommodated by regeneration of some chelated phosphate ester from the monodentate ester complex in competition with the cleavage of the ester ligand from the Co(III) ion. Alternatively attack by coordinated OH^- at the phosphorus atom could be invoked. However, this reaction was much slower than the direct hydrolysis of the chelate and it was not investigated further. The rate remains linear in OH^- even at high base concentrations, but the yields of nitrophenolate ion begin to fall off at the upper level. The implication is that either a higher order term begins to appear for the conjugate base path or for decomposition of the five-coordinate phosphorane intermediate. There has been no sign of higher order terms for the conjugate base mechanism leading to cleavage of a ligand–metal bond and this path is therefore unlikely. However the phosphorane intermediate could bifurcate in the high base concentrations by deprotonation, to open the chelate as well as cleave the ester. Such a route would fit the rate and stoichiometry data, provided decomposition of the intermediate is not rate determining. A six-coordinate intermediate is also possible with the same restriction. The deviation is interesting but difficult to study by the tracer technique, since only a small fraction of the total

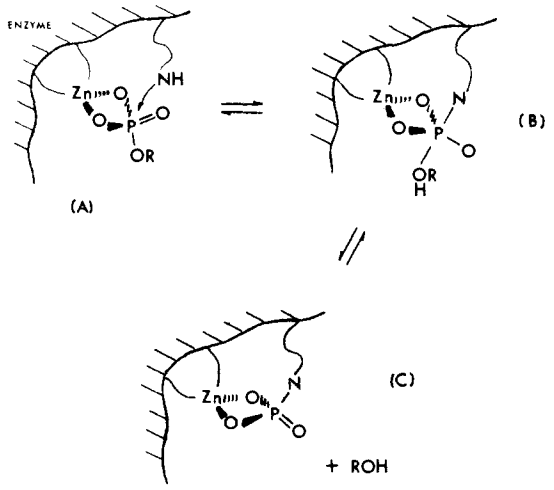

Figure 7. A possible mechanism for the catalytic action of the metal ion in alkaline phosphatase.

reaction is involved. However, some evidence for ring opening via O-P rupture might be adduced from the experiments of Lincoln and Stranks[44] with base hydrolysis of chelated PO_4^{3-} ion. Ring opening in basic solution occurred with 35% P-O rupture and 65% Co-O rupture to give the monodentate phosphate ion. It seems reasonable to argue that both the five-coordinate P intermediate path and the conjugate base hydrolysis path are being observed in this instance also, and the tracer in the PO_4^{3-} ion could come from ring opening in the chelated phosphate.

The hydrolysis data for the free ester ligand in the presence of a large excess of $[Co(tn)_2(OH)(OH_2)]^{2+}$ ion at pH 7.54 are consistent with the data for the chelate provided we assume all the ligand is chelated. In this pH region H_2O exchange between complex and solvent should maximize and estimates indicate it is very fast, $t_{1/2} < 1$ s,[8] in fact unusually fast compared with *cis*- or *trans*-$[Co(en)_2(OH)(OH_2)]^{2+}$ ion.[45] Cis-trans rearrangement is correspondingly rapid[8] in this condition and entry of ligands and rearrangement could therefore be rapid compared with hydrolysis of the chelated ester. At higher pH values the rate of hydrolysis falls off and this could be ascribed to a depreciation in the capture of the free ligand. Both the dihydroxo and diaquo ions would be expected to exchange oxygen with the solvent more slowly than the hydroxo aqua ion and there is some evidence for such an effect in Table I.

A revealing result in this context was the hydrolysis rate when the hydroxo aqua complex and ester were present in comparable concentrations (10^{-4} M). Under these conditions little or no hydrolysis was observed. The inference is that at these low concentrations the capture and chelation of the ester are not comparable with the rate observed for hydrolysis of the chelate and that once the ligand is lost from the metal ion it is not regained in the lifetime of the chelated ester hydrolysis.

An apparent inconsistency is the equality of the rates of hydrolysis for the chelated nitrophenylphosphate and $[Co(tn)_2(OH)(OH_2)]^{2+}$ plus nitrophenylphosphate at pH 7.5 coupled with yields of nitrophenol of 38 and 100%, respectively. The results imply that under these pH conditions equilibration between free, monodentate, and chelate ester is faster than chelate hydrolysis. Such a result seems inconsistent with the data at high pH where monodentate nitrophenylphosphate hydrolyzes slowly to nitrophenol. However, it could arise if aqua and hydroxo ions were the reactants under the different conditions. If the product ratios of nitrophenol, monodentate ester, and free ester are constant over the pH range studied then a substantial amount of monodentate should be observed even after $20t_{1/2}$. However, at pH 7.5 hydrolysis of the chelated ester showed little monodentate nitrophenylphosphate after $3t_{1/2}$, (~3%). This implies that the aqua monodentate cyclizes or loses ester at pH 7.5 faster than it hydrolyzes, whereas the hydroxo complex is comparatively unreactive.

Although an x-ray crystallographic study on *E. coli* alkaline phosphatase has been commenced,[46] the structure is only known at the moment to a 7.7 Å resolution. However, it can be seen that large channels exist in the crystalline structure which would allow substrates to diffuse to the bound Zn^{2+} ions. Other studies reviewed in an article by Reid and Wilson[47] have shown that Zn^{2+} or other divalent metal ions activate the enzyme. Also there are indications that phosphate binds through the metal ion in the enzyme. In keeping with a suggestion by Spiro,[48] the present study would support a role for the Zn^{2+} binding the phosphate residue as a chelate in order to activate the substrate, Figure 7. An adjacent nucleophile N attached to the enzyme, e.g.,$-CH_2OH$, $-CH_2SH$, imidazole, could then readily attack the P atom to give the strain relieved intermediate (B), which decomposes to the alcohol ROH and the phosphorylated enzyme. The last appears as an established feature of this enzymic system. The rationale leaves the phosphate residue still in an activated state attached to the Zn^{2+} ion and susceptible to a new nucleophile to give trans phosphorylation or to a water molecule to release phosphate ion.

A similar role for activation by the metal ion could be envisaged for phosphotransferases and even in oxidative phosphorylation.

References and Notes

(1) On leave from Boston University, Boston, Mass., as Visiting Fellow at The Australian National University, 1974-1975.
(2) M. Tetas and J. M. Lowenstein, *Biochemistry*, **2**, 353 (1963).
(3) F. J. Farrell, W. A. Kjellstrom, and T. G. Spiro, *Science*, **164**, 320 (1969); J. MacB. Harrowfield and A. M. Sargeson, unpublished work.
(4) J. J. Steffens, E. J. Sampson, I. S. Sievers, and S. J. Benkovic, *J. Am. Chem. Soc.*, **95**, 936 (1973).
(5) P. Gillespie, F. Ramirez, I. Ugi, and D. Marquarding, *Angew. Chem., Int. Ed. Engl.*, **12**, 91 (1973).
(6) A. S. Mildvan and C. M. Grisham, *Struct. Bonding (Berlin)*, **20**, 1 (1974).
(7) (a) E. A. Dennis and F. H. Westheimer, *J. Am. Chem. Soc.*, **88**, 3422 (1966); (b) F. H. Westheimer, *Acc. Chem. Res.*, 1 70 (1968).
(8) I. R. Jonasson, R. S. Murray, D. R. Stranks, and J. K. Yandell, *Proc. Int. Conf. Coord. Chem., 12th*, 32 (1969); I. R. Jonasson, S. F. Lincoln, and D. R. Stranks, *Aust. J. Chem.*, **23**, 2269 (1970); D. R. Stranks, private communication.
(9) O. A. Bessey and R. H. Love, *J. Biol. Chem.*, **196**, 175 (1952).
(10) A. M. Sargeson and H. Taube, *Inorg. Chem.*, **5**, 1094 (1966).
(11) The Busing and Levy programs for four-circle diffractometers, *Acta Crystallogr.*, **22**, 452 (1967), were used for all phases of diffractometer control and data collection.
(12) Here and throughout the crystallography sections (apart from Figure 2) the uncertainties given in parentheses are estimated standard deviations in the least significant figures quoted.
(13) J. De Meulenaer and H. Tompa, *Acta Crystallogr.*, **19**, 1014 (1965).
(14) $\sigma(I) = [CT + (Tp/Tb)^2 (B_1 + B_2)]^{1/2}$ where CT is the integrated peak intensity counted for Tp seconds and B_1 and B_2 are the background intensities each measured for Tb/2 seconds.
(15) All computations were carried out on the Australian National University Univac 1108 computer using the ANUCRYS set of crystallographic programs compiled and developed by Drs. P. O. Whimp and D. M. Taylor.
(16) D. T. Cromer and J. T. Waber, *Acta Crystallogr.*, **18**, 104 (1965).
(17) D. T. Cromer, *Acta Crystallogr.*, **18**, 17 (1965).
(18) Standard deviations for each structure amplitude were calculated as $\sigma(F_o) = \{[\sigma(I)/Lp]^2 + (\rho|F_o|^2)^2\}^{1/2}/2|F_o|$, where Lp is appropriate Lorentz and polarization correction and $\rho(0.032)$ is an instrumental uncertainty constant.
(19) R. F. Stewart, E. R. Davidson, and W. T. Simpson, *J. Chem. Phys.*, **42**, 3175 (1965).
(20) M. R. Churchill, *Inorg. Chem.*, **12**, 1213 (1973).
(21) B. F. Anderson, D. A. Buckingham, G. J. Gainsford, G. B. Robertson, and A. M. Sargeson, *Inorg. Chem.*, **14**, 1658 (1975).
(22) D. Witiak, J. C. Clardy, and D. S. Martin, *Acta Crystallogr., Sect. B*, **28**, 2694 (1972).
(23) A. R. Gainsford, D. A. House, and W. T. Robinson, *Inorg. Chim.Acta*, **5**, 595 (1971).
(24) D. A. Buckingham, G. J. Gainsford, W. T. Robinson, and A. M. Sargeson, personal communication.
(25) Orthogonalized coordinates X, Y, and Z are given by: $X = 12.2070x + 0.1683y + 0.1849z$; $Y = 9.1800y + 5.2350z$; $Z = 10.8388z$.
(26) R. J. Geue and M. R. Snow, *J. Chem. Soc. A*, 2981 (1971); G. A. Barclay and B. F. Hoskins, *J. Chem. Soc.*, 586 (1962).
(27) K. Kaas and A. M. Sorensen, *Acta Crystallogr.*, **29**, 113 (1973).
(28) J. A. Bertrand and T. C. Hightower, *Inorg. Chem.*, **12**, 206 (1973).

(29) T. A. Steitz and W. M. Lipscomb, *J. Amer. Chem. Soc.*, **87**, 2488 (1965).
(30) C. L. Coulter, *J. Am. Chem. Soc.*, **95**, 570 (1973).
(31) S. Furberg and J. Solbakk, *Acta Chem. Scand.*, **27**, 1226 (1973).
(32) F. S. Ezra and R. L. Collin, *Acta Crystallogr., Sect. B*, **29**, 1398 (1973).
(33) L. Giarda, F. Garbossi, and M. Calcaterra, *Acta Crystallogr., Sect. B*, **29**, 1826 (1973).
(34) F. H. Westheimer, *Acc. Chem. Res.*, **1**, 70 (1968), and references cited therein.
(35) R. Kluger, E. Clovitz, E. Dennis, L. D. Williams, and F. H. Westheimer, *J. Am. Chem. Soc.*, **91**, 6066 (1969).
(36) For a summary of relevant data see R. K. Osterheld, *Top. Phosphorus Chem.*, 7, 191-192 (1972).
(37) (a) F. Ramirez and I. Ugi, *Bull. Soc. Chim. Fr.*, 453 (1974); (b) H. G. Khorana, G. M. Tener, R. S. Wright, and J. G. Moffatt, *J. Am. Chem. Soc.*, **79**, 430 (1957); (c) E. Cherbuliez, H. Probst, and V. Rabinowitz, *Helv. Chim. Acta*, **42**, 1377 (1959).
(38) By analogy with $(en)_2CoPO_4$, it would be expected that $(tn)_2CoPO_4$ would be a considerably weaker base than 4-nitrophenolate anion: see S. F. Lincoln and D. R. Stranks, *Aust. J. Chem.*, **21**, 57 (1968).
(39) A. S. Mildvan and C. M. Grisham, *Struct. Bonding (Berlin)*, **20**, 1-22, (1974).
(40) The rate of attack of hydroxide ion on *N*-acetylimidazole, for example, is accelerated only ~20-fold when the heterocycle is coordinated in a tripositive complex: see J. M. Harrowfield, V. Norris, and A. M. Sargeson, *J. Am. Chem. Soc.*, **98**, 7282 (1976).
(41) J. A. Bertrand and T. C. Hightower, *Inorg. Chem.*, **12**, 206 (1973); U. Thewalt and R. E. Marsh, *Inorg. Chem.*, **10**, 1789 (1971); K. Wieghardt, J. Weiss, and H. Siebert, *Z. Anorg. Allg. Chem.*, **383** 151 (1971); U. Thewalt and R. E. Marsh, *J. Am. Chem. Soc.*, **89**, 6364 (1967); C. K. Prout, *J. Chem. Soc.*, 4429 (1962).
(42) M. Iwata and Y. Saito, *Acta. Crystallogr., Sect. B*, **29**, 822 (1973).
(43) R. D. Spratley, W. C. Hamilton, and J. Ladell, *J. Am. Chem. Soc.*, **89**, 2272 (1967).
(44) S. F. Lincoln and D. R. Stranks, *Aust. J. Chem.*, **21**, 37, 57, 67 (1968).
(45) W. Kruse and H. Taube, *J. Am. Chem. Soc.*, **83**, 1280 (1961).
(46) J. R. Knox and K. W. Wyckoff, *J. Mol. Biol.*, **74**, 533 (1973).
(47) T. W. Reid and I. B. Wilson, *Enzymes, 3rd Ed.*, **4**, Chapter 17 (1971).
(48) T. G. Spiro in "Inorganic Biochemistry", G. L. Eichorn, Ed., Elsevier, New York, N.Y., 1973, Chapter 17.

On the Alkaline Hydrolysis of β-Dicarbonyl Compounds

J. Rahil and R. F. Pratt*

Contribution from the Department of Chemistry, Wesleyan University, Middletown, Connecticut 06457. *Received February 26, 1976*

Abstract: A recent report[3] in this journal proposed that modification of the classical Pearson and Mayerle[2] mechanism for hydrolysis of β-dicarbonyl compounds was required in the case of substituted aroylacetaldehydes. The modification suggested involved proton transfer from a ketone hydrate hydroxyl group to hydroxide ion as rate limiting under some circumstances. We have shown by NMR measurements that rates of exchange and hydrolysis of benzoylacetaldehyde in $NaOD/D_2O$ solutions are comparable so that a more likely modification has the first step, proton transfer from water to carbon in forming the dicarbonyl compound from its enolate, of primary importance in determining the rate of alkaline hydrolysis of these compounds.

Many reactions of biological importance involving the formation or cleavage of carbon-carbon bonds can be seen to occur formally by the addition or displacement of a carbanion to or from a carbonyl center (eq 1 and 2). Of these reactions

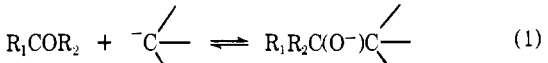

(1)

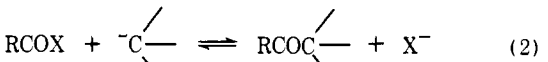

(2)

the first is illustrated most clearly by reactions catalyzed by the aldolase enzymes and the latter by those catalyzed by enzymes of fatty acid metabolism, the β-ketoacyl synthases (forward reaction) and the thiolases (reverse). The function and mechanisms of action of these enzymes have been recently reviewed.[1]

One model system (to the reverse of eq 2) that has been examined in some detail is that of the alkaline hydrolysis of β-dicarbonyl compounds.

$$R_1COCR_2R_3COR_4 + OH^-(H_2O) \rightarrow R_1CO_2^- + R_2R_3CHCOR_4$$

These reactions have, of course, also been of significant importance in synthetic organic chemistry.

The commonly accepted mechanism of these cleavage reactions, involving rate-determining breakdown of carbonyl hydrate species, was proposed many years ago by Pearson and Mayerle for acetylacetone derivatives[2] (Scheme I).

Scheme I

$$RCOCH_2COR \overset{K_a}{\rightleftharpoons} RCOCH{=}CRO^- + H^+ \quad (3)$$

$$RCOCH_2COR + OH^- \overset{K_1}{\rightleftharpoons} RCOCH_2C(OH)(O^-)R \xrightarrow{k_1} RCOCH_3 + RCO_2^-$$

$$RCOCH_2C(OH)(O^-) + OH^- \rightleftharpoons RCOCH_2C(O^-)_2R \xrightarrow{k_2} RCOCH_3 + RCO_2^-$$

Recently in this journal report[3] was made of one such cleavage, that of aroylacetaldehydes, where kinetic analysis suggested that a variant of this mechanism must obtain; Scheme II was proposed.

Scheme II

$$ArCOCH_2CHO \overset{K_a}{\rightleftharpoons} ArCOCH{=}CHO^- + H^+$$

$$ArCOCH_2CHO + H_2O \overset{K_H}{\rightleftharpoons} ArCH_2CH(OH)_2$$

$$\overset{k_1[OH^-]}{\underset{k_{-1}}{\rightleftharpoons}} ArCOCH_2CH(OH)O^-$$

$$ArCOCH_2CHO + OH^- \overset{k_2}{\underset{k_{-2}}{\rightleftharpoons}} ArCOCH_2CH(OH)O^-$$

$$ArCOCH_2CH(OH)O^- + OH^- \xrightarrow{k_3} ArCOCH_3 + HCO_2^-$$

The authors incorporated a proton transfer step to oxygen which could become rate determining under certain circumstances, treated $ArCOCH_2CH(OH)O^-$ as a steady state in-